Nonlinear optical properties of lead sulfide nanocrystals in polymeric coatings

S W Lu[1], U Sohling, M Mennig and H Schmidt

Institut für Neue Materialien, gem. GmbH, Gebäude 43, Im Stadtwald, D-66123, Saarbrücken, Germany

E-mail: songweilu@hotmail.com

Abstract

Lead sulfide (PbS) nanocrystals with a particle size of 3.3 ± 0.7 nm have been synthesized in a poly vinyl alcohol (PVA) coating on fused silica glass substrates. The coating was dip-coated from a PVA aqueous solution, in which PbS nanocrystals were precipitated and stabilized in the polymer matrix. Third-order nonlinear optical susceptibility of PbS nanocrystals is dependent on the wavelength with its maximum located near the first excitonic absorption peak resulting from the quantum confinement effect, according to the results of degenerate four wave-mixing. This suggests an enhancement of the nonlinear optical property by excitonic resonance. The maximum figure of merit, $\chi^{(3)}/\alpha$, is as high as 2.91×10^{-12} esu m as measured at 595 nm.

1. Introduction

Linear and nonlinear optical properties of semiconductor quantum dots have attracted extensive research interest over recent years [1–8]. Due to their promising applications in the field of optical computing, materials with a large nonlinear optical susceptibility and a fast response time are required [9]. Lead sulfide (PbS) nanoparticles are of particular interest because of their fine structured optical absorption and expected large third-order nonlinear optical susceptibility [10, 11]. It is predicted that for a given size the nonlinearities of PbS nanocrystals will be much larger than that of other semiconductor quantum dots such as GaAs and CdS [2, 10]. However, most investigations have dealt with the interesting fine structured linear optical properties of PbS quantum dots [12–14]. Although there are several research papers reporting third-order nonlinear optical susceptibilities of PbS nanoparticles, their $\chi^{(3)}$ values were not large or the sample was liquid without any practical applications [15–19]. The following values have been reported: a $\chi^{(3)}$ value of 1.1×10^{-6} esu from CdS doped glasses [20], a $\chi^{(3)}/\alpha$ value, the figure of merit, as high as 1.9×10^{-11} esu m from CuCl doped glasses [21] and 1.6×10^{-11} esu m from 2 mm thick $CdS_{0.9}Se_{0.1}$ glasses [1]. On the other hand, a $\chi^{(3)}$ value was reported of about 1.0×10^{-8} esu from PbS nanoparticles in polymer matrices [16]. From a solution of PbS colloids stabilized with sodium dioctyl sulfosucinate in reverse micelles, a $\chi^{(3)}/\alpha$ value of 7.2×10^{-14} esu m was reported [18]. Guo and Ai [19] reported a $\chi^{(3)}/\alpha$ value of 8.4×10^{-15} esu m from PbS nanocrystals modified with sodium dodecyl benzene sulfonate.

It is obvious that there is a gap between the theoretical predictions and the reported data of the nonlinear optical susceptibility of PbS nanoparticles. The objective of this research is to focus on the synthesis of PbS nanoparticles with an extremely narrow size distribution in solid matrices, in the hope that the new nanomaterial will exhibit a fine structured linear optical property and a large third-order nonlinear optical susceptibility. The nanostructures, linear and nonlinear optical properties of poly vinyl alcohol (PVA)-stabilized PbS nanoparticles are investigated in detail.

2. Experimental details

A total of 5 ml 5.0 wt% PVA (molecular weight 9000–10 000, 80% hydrolyzed, Aldrich Chemical Company) aqueous solution, 2.5 ml aqueous solution of 0.01 M $Pb(ClO_4)_2$ (50% in water, 1.7 M, Fluka), and 42.5 ml of distilled water were mixed together while stirring at 0 °C in a glass flask and slowly bubbled with N_2 gas. After stirring for 30 min, the

[1] Present address: PPG Industries, Inc., Glass Technology Center, PO Box 11472, Pittsburgh, PA 15238-0472, USA.

flask was sealed from ambient atmosphere. This was followed by injecting 2.0 ml of H_2S gas into the above mixture within 2 min using a 2 ml plastic syringe. Consequently, deep wine-red colloidal PbS was formed *in situ* in the solution. Extra H_2S gas was bubbled out with N_2 gas for 10 min. Polymeric coatings were multiply dip-coated on pre-cleaned fused silica glass substrates from the above solution at a withdrawal rate of 6 mm s^{-1}. The as-prepared coatings were transparent orange in colour. The coatings were then cured in N_2 atmosphere at 120 °C for 2 h.

High-resolution transmission electron microscope (HRTEM) investigations were performed using a Philips CM 200 FEG transmission electron microscope with a Schottky type field emission gun (FEG) generating the beam energy up to 200 keV. The film thickness was measured by means of a Tencor P-10 surface profiler instrument. Absorption spectra were recorded at room temperature using a Hitachi U-3000 spectrophotometer accompanied by a 2 mm fused silica cuvette and referred by air. Third-order nonlinear optical susceptibility $\chi^{(3)}$ of PbS nanoparticles was measured by a degenerate four-wave mixing (DFWM) method at room temperature in ambient atmosphere. An excimer pumped tunable dye laser was used as a pump source by adjusting the beam wavelength from 585 to 630 nm. The pulse time was 25 ns and the laser power intensity was $\geqslant$50 kW cm^{-2}. The DFWM signal was detected by a gated intensified detector (response time <100 ns).

3. Results and discussion

3.1. Nanostructures

In figure 1 we show an HRTEM image of PbS nanoparticles homogeneously distributed in PVA coatings on fused silica glass substrates after drying at 120 °C for 2 h in N_2. The individual particle in figure 2 is of elliptical with its width to length ratio of 2:3. The Gaussian distribution of PbS nanoparticles in polymer coatings as statistically estimated from approximately 300 particles from the HRTEM image in figure 1 is presented in figure 3. The mean particle size of PbS quantum dots in a PVA matrix is statistically estimated to be 3.3 nm with a narrow standard deviation of ±0.7 nm. The calculated crystalline constant d is 0.297 nm for the (200) face, which is in good agreement with the crystalline lattice constant of cubic PbS (JCPDS No 5–592 cubic PbS, $d(200) = 0.297$ nm).

The elliptical form of the PbS nanoparticle from the HRTEM investigation may be either prolate (i.e., rod-like) or oblate (i.e., disk-like). According to Gacoin *et al* [7], the formation and growth of PbS nanoparticles during precipitation could be interpreted that, in the initial step just after the addition of H_2S or $Pb(ClO_4)_2$, the particles are formed as small nuclei that are spherical in shape. Then the growth process is first anisotropic and leads to particles having a rod-like shape. Finally, further growth of the crystal leads to more isotropic particles that tend to become cubic. This indicates that the growth of PbS nanoparticles is very sensitive to colloidal preparation conditions. The PbS nanoparticles precipitated in this research have an elliptical form with a width to length ratio of about 2:3, resulting from the injection of excess H_2S gas to a solution, where Pb^{2+} is surrounded by

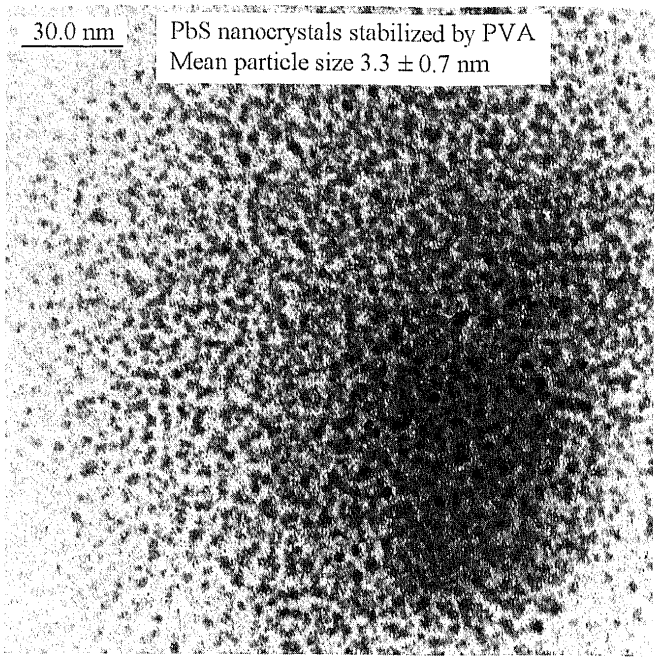

Figure 1. HRTEM image of PbS nanoparticles from PbS–PVA coatings after heat treatment at 120 °C for 2 h in N_2.

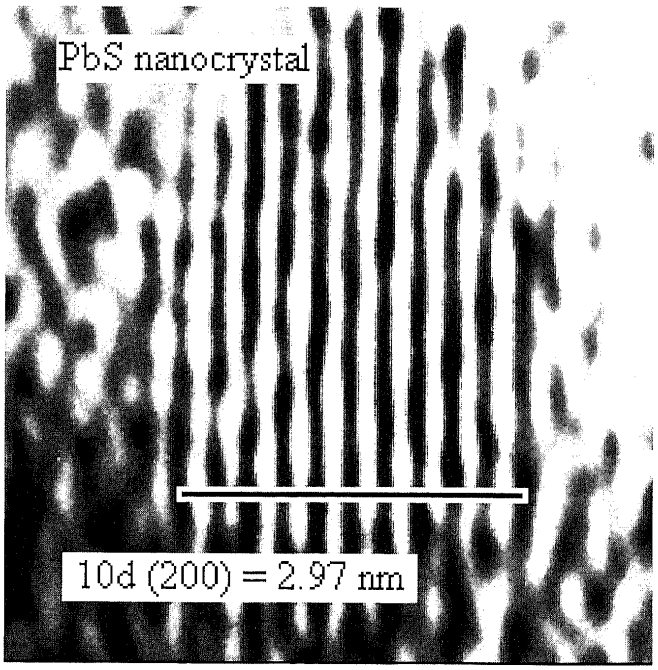

Figure 2. An individual PbS nanocrystal as observed by HRTEM investigation. The particle is elliptical with a width to length ratio of 2:3.

PVA, and the precipitation of PbS nanoparticles at 0 °C by preventing the anisotropic growth of PbS nanoparticles. It has been reported that rod-like PbS particles 18 nm long with a diameter of 1.5–2.5 nm (i.e., width to length ratio about 1:7.2–1:12) have been observed from solutions containing 4×10^{-4} M PbS stabilized by 3×10^{-3} M PVA [12]. In their work, PbS nanoparticles were precipitated by the injection of excess $Pb(ClO_4)_2$ aqueous solutions, where Pb^{2+} was not surrounded by a stabilizer, to H_2S gas saturated PVA aqueous solutions, leading to particles with a width to length ratio of 1:7.2–1:12 resulting from the lower inhibition of the anisotropic growth during precipitation. The anisotropic growth of PbS

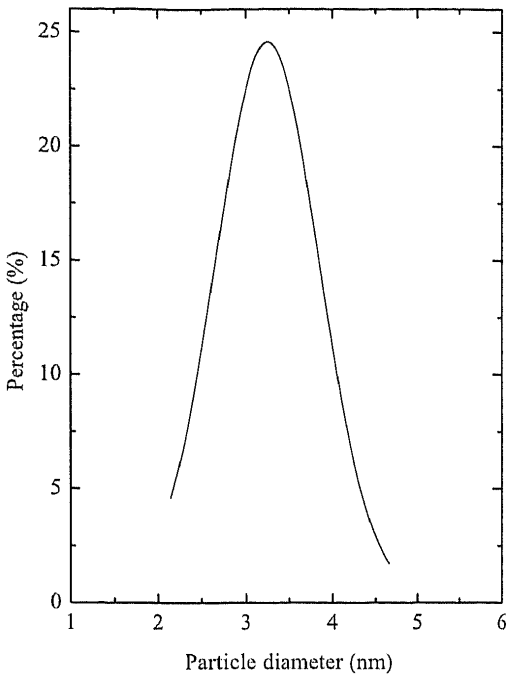

Figure 3. The Gaussian distribution of PbS nanoparticle size in PVA coatings after curing at 120 °C for 2 h in N_2, as estimated from HRTEM images. The mean particle diameter is 3.3 ± 0.7 nm.

nanoparticles during precipitation was supported by the results of Gacoin *et al* [7] that PbS nanoparticles precipitated in methanol without a stabilizer followed by the addition of 3-mercaptopropyl triethoxysilane and $Zn(NO_3)_2$ revealed both cubic forms with a size of about 13 nm and rod-like forms with characteristic dimensions of about 2.5 and 25 nm (i.e., the width to length ratio of 1:10) due to the lack of a stabilizer in methanol during precipitation. Erce-Montilla *et al* [8] also observed spherical and cubic PbS nanoparticles ranging from 6.5 to 10.5 nm, and needle-like particles 7 nm wide and 15–20 nm long due to different concentrations of PbS and a surface capping agent. Thus, it is very likely that PbS nanoparticles with near-spherical forms are produced only in a better-stabilized medium, such as a PVA aqueous solution with homogeneously distributed lead ions anchored by PVA polymeric chains in this work.

3.2. *Linear optical property*

The absorption spectrum of PbS nanocrystals in a PVA aqueous solution prepared at 0 °C is demonstrated in figure 4. The as-prepared solution exhibits three sharp peaks at 592, 391, and 294 nm resulting from the quantum confinement effect [7, 10, 12]. A PbS–PVA coating still reveals three fine structural peaks after dipping in the above solution and curing at 120 °C for 2 h in a N_2 atmosphere (figure 4). Nevertheless, the shape and the intensity ratio of the peaks are slightly different from the PbS colloidal solution. All absorption peaks become broader in the PbS–PVA coatings than in the PbS–PVA aqueous solution. In addition, the absorption peak at 391 nm drops faster than other peaks comparing the coating to the solution. This is possibly due to the further growth of PbS nanoparticles during dipping and curing, resulting in a broadening of the particle size distribution, an increase in particle size, and/or an increase in the surface defects, possibly as a result of Ostwald ripening.

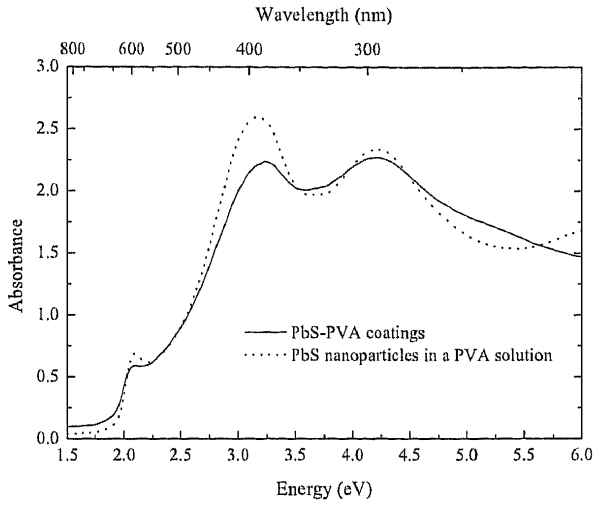

Figure 4. The absorption spectra of 5 × 10^{-4} M PbS colloidal aqueous solutions stabilized by 0.5 wt% PVA and of a PbS–PVA coating on a fused silica glass substrate after curing at 120 °C for 2 h in N_2.

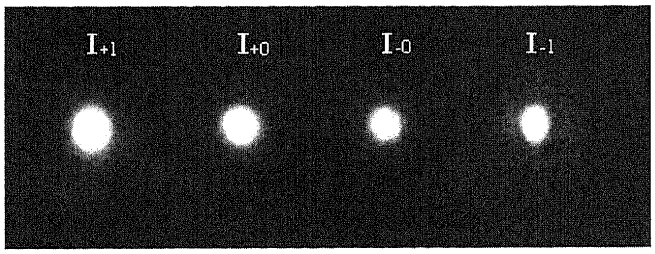

Figure 5. A photograph of linear signals (I_{+0} and I_{-0}, with filter) and nonlinear signals (I_{+1} and I_{-1}).

3.3. *Nonlinear optical property*

Figure 5 shows a direct observation of both linear signals (I_{+0} and I_{-0}, with filter) and nonlinear signals (I_{+1} and I_{-1}) from a PbS–PVA coating in a dark room. The nonlinear signals come from a change of the refractive index, i.e. the addition of an nonlinear refractive index to the linear refractive index, of the PbS–PVA coating under two incident beams with the same frequency.

The third-order nonlinear optical susceptibility $\chi^{(3)}$ can be calculated from the nonlinear signal detected as represented in equation (1) [22]

$$\chi^{(3)} = \frac{4n^2 c\varepsilon_0 \lambda \alpha \sqrt{\eta}}{3\pi(1-T)I_p} \tag{1}$$

$$\eta = I_1/I_0 \tag{2}$$

where n is the linear refractive index, c the velocity of light, λ the measurement wavelength, α the sample absorption coefficient at λ, I_p the pump intensity, T the transmission at I_p, ε_0 the dielectric constant of the material. Here, η is the diffraction efficiency (equation (2)), i.e., the intensity relation of the transmitted first-order (I_1) and zeroth order (I_0) of the diffraction pattern, which appears by self-diffraction of a laser induced grating. The value $\chi^{(3)}/\alpha$ is, therefore, a figure of merit that can be used for the evaluation of nonlinear optical properties among different materials, assuming the same measurement conditions. Although $\chi^{(3)}/\alpha$ is defined to be a figure of merit for a resonant effect to eliminate

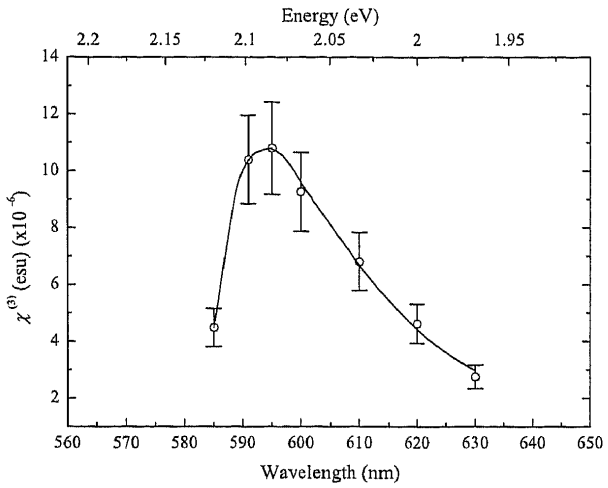

Figure 6. The wavelength dependence of $\chi^{(3)}$ of a 500 nm thick PbS–PVA coating on a fused silica glass substrate.

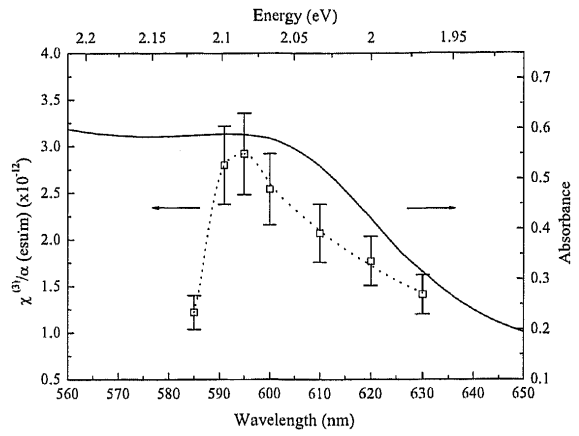

Figure 7. The wavelength dependence of $\chi^{(3)}/\alpha$ and the corresponding absorption spectrum of a 500 nm thick PbS–PVA coating on a silica glass substrate after heating at 120 °C for 2 h in a N_2 atmosphere.

the influence of the sample thickness and the concentration of nonlinear species, it still depends on measurement of the wavelength according to equation (1).

As shown in figures 6 and 7, the third-order nonlinear optical susceptibility $\chi^{(3)}$ and its figure of merit, $\chi^{(3)}/\alpha$, increase with the wavelength from 585 nm, and reach their maxima of 1.06×10^{-5} esu and 2.91×10^{-12} esu m, respectively, at 595 nm. Thereafter, the nonlinearities decrease as the wavelength increases up to 630 nm. It is obvious that the optical nonlinearity reaches its maximum around the first-order excitonic peak located at 592 nm. It should be noted that the wavelength dependence of $\chi^{(3)}/\alpha$ is similar to the absorption spectrum (figure 7). In the absorption spectrum, the maximum absorbance is located at 592 nm, while in the $\chi^{(3)}/\alpha$ spectrum, its maximum is found at 595 nm. In the wavelength region that is longer than the excitonic resonance, both the absorbance and $\chi^{(3)}/\alpha$ values decrease. In the wavelength region that is shorter than the excitonic resonance, the $\chi^{(3)}/\alpha$ value drops dramatically, while the absorbance first drops and then increases further as the wavelength decreases. This is primarily caused by the background resulting from the scattering of small particles, and the contribution of another peak at 391 nm, since the long tail of this 391 nm peak extends to the wavelength region of the first excitonic peak (figure 4). Hence, the figure of merit $\chi^{(3)}/\alpha$ is governed by the first-order excitonic transition, i.e., the $1s_h \rightarrow 1s_e$ transition, indicating the resonant enhancement of the nonlinear optical properties with the confined exciton. This phenomenon has already been observed from CdS doped glasses [23], CdS_xSe_{1-x} doped glasses [24], CuBr quantum dots in glasses [25], Au nanoparticle doped SiO_2 thin films [26], and Cu nanoparticle doped SiO_2 thin films [27].

According to theoretical calculations [2], it is expected that, in the case of a strong quantum confinement effect, such as PbS quantum dots, a large third-order nonlinear susceptibility will be obtained. In such a case, the radii R of nanoparticles, e.g. 1.65 ± 0.35 nm in the PVA coating, are much smaller than the Bohr radii of both the electron and the hole, i.e., 9 nm for PbS [28, 29]. As a result, the Coulomb energy may be neglected in comparison with the strong confinement energy. However, it is important that a large nonlinear optical susceptibility will be expected only in the case of an extremely narrow size distribution [2]. The broadening of the particle size distribution will give rise to a reduction in the optical nonlinearities [2]. In this work, the particles are in elliptical forms with a width to length ratio of 2:3 according to HRTEM results, and have a small size distribution of ± 0.7 nm. The width to length ratio of 2:3 of the elliptical particles in this work is much smaller than that of PbS nanoparticles prepared by Gallardo *et al* [12] and Gacoin *et al* [7]. The size distribution of PbS nanoparticles in a PVA matrix is smaller than that of PbS nanoparticles in a reverse micelle solution, from which there is no fine structured absorption [18, 30]. Therefore, the small ratio of width to length and the narrow size distribution may be the important factors in the enhancement of the third-order nonlinear optical susceptibility of PbS nanoparticles in PVA coatings. Moreover, the homogeneous distribution of the quantum dots in a matrix is another key point of the enhanced nonlinearities. In addition, the surface defects on quantum dots may play an important role in the linear and nonlinear optical properties. These effects lead to the enhancement of third-order nonlinear optical susceptibility around the excitonic transition. In this research, the figure of merit is 43 times larger than the reported value of PbS nanoparticles in a reverse micelle solution measured at 532 nm.

To summarize, the enhancement of the optical nonlinearities results from a small elliptical particle with small ratio of width to length, an extremely narrow size distribution, low surface defect, and homogeneous dot distribution in a matrix. The enhancement of the $\chi^{(3)}/\alpha$ value may benefit from surface modification of the quantum dots. Both the $\chi^{(3)}$ and $\chi^{(3)}/\alpha$ spectra exhibit an enhancement near the first excitonic peak due to the confined exciton.

4. Conclusions

PbS quantum dots with a mean size of 3.3 ± 0.7 nm have been successfully synthesized in aqueous solutions in the presence of PVA as stabilizer and in coatings by a dipping coating and a post-curing. Both PbS–PVA aqueous solutions and coatings exhibit three fine structured absorption peaks caused by the quantum confinement effect. Third-order nonlinear optical susceptibility $\chi^{(3)}$ is dependent on the wavelength with its maximum located at 595 nm, enhanced by the first-order

excitonic transition. The figure of merit, $\chi^{(3)}/\alpha$, of about 2.91×10^{-12} esu m is two orders of magnitude larger than that of Au nanoparticle implanted silica glasses, three times larger than that of Au nanoparticle doped Ormocer thin films, and 43 times larger than that of PbS in solution. The enhancement of the third-order nonlinear optical susceptibility is a result of small nanocrystallite size and extremely narrow size distribution, low surface defects, and homogeneous distribution of particles in the coatings.

Acknowledgments

S W Lu would like to sincerely thank G Jung and U Becker for the nonlinear optical measurements and useful discussion, and Th Krajewski for the high-resolution TEM investigations.

References

[1] Jian R K and Lind R C 1983 *J. Opt. Soc. Am.* **73** 647
[2] Banyai L, Hu Y Z, Lindberg M and Koch S W 1988 *Phys. Rev.* B **38** 8142
[3] Alivisatos A P 1995 *Mater. Res. Soc. Bull.* **20** 23
[4] Colvin V L, Schlamp M C and Alivisatos A P 1994 *Nature* **370** 354
[5] Nogami M, Nagasaka K and Kotani K 1990 *J. Non-Cryst. Solids* **126** 87
[6] Guglielmi M, Martucci A, Righini G and Pelli S 1994 *Sol–Gel Optics III (SPIE vol 2288)* p 174
[7] Gacoin T, Boilot J B, Gandais M, Ricolleau C and Chamarro M 1995 *Mater. Res. Soc. Symp. Proc.* vol 358 p 247
[8] Erce-Montilla R, Pinero M, De la Rosa-Fox N, Santos A and Esquivias L 2001 *J. Mater. Res.* **16** 2572
[9] Kadono M A K, Haruta M, Sakaguchi T and Miya M 1995 *Nature* **374** 625
[10] Machol J L, Wise F W, Patel R C and Tanner D B 1993 *Phys. Rev.* B **48** 2819
[11] Martucci A, Fick J, Schell J, Battaglin G and Guglielmi M 1999 *J. Appl. Phys.* **86** 79
[12] Gallardo S, Gutierrez M, Henglein A and Janata E 1989 *Ber. Bunsenges. Phys. Chem.* **93** 1080
[13] Nenadovic M T, Comor M I, Vasic V and Micic O I 1990 *J. Phys. Chem.* **94** 6390
[14] Nedeljkovic J M, Patel R C, Kaufman R, Pruden C J and O'Leary N 1993 *J. Chem. Educ.* **70** 342
[15] Zhao J, Jin C, Zhou F, Qin W, Dou K, Gao Y, Huang S and Yu J 1992 *Int. Conf. on Physics and Semiconductor (Singapore)* vol 21 p 1860
[16] Gao M, Yang Y, Yang B, Bian F and Shen J 1994 *J. Chem. Commun.* 2779
[17] Moriguchi I, Hanai K, Teraoka Y, Kagawa S, Yamada S and Matsuo T 1995 *Japan. J. Appl. Phys.* **34** L323
[18] De Sanctics O, Kadono K, Tanaka H and Sakaguchi T 1995 *Mater. Res. Soc. Symp.* vol 358 p 253
[19] Guo L and Ai X 2000 *Mater. Chem. Phys.* **63** 30
[20] Takada T, Mackenzie J D, Yamane M, Kang K, Peyghambarian N, Reeves R J, Knobbe E T and Powell R C 1996 *J. Mater. Sci.* **31** 423
[21] Kondo Y, Kuroiwa Y, Sugimoto N, Manabe T, Ito S, Tokizaki T and Nakamura A 1996 *J. Non-Cryst. Solids* **196** 90
[22] Horan P, Blau W, Byrne H and Berglund P 1990 *Appl. Opt.* **29** 31
[23] Nogami M 1993 *Sol–Gel Optics: Processing and Applications* (Boston: Kluwer)
[24] Ricard D, Roussignol P, Hache F and Flytzanis Ch 1990 *Phys. Status Solidi* b **159** 275
[25] Li Y, Takata M and Nakamura A 1998 *Phys. Rev.* B **57** 9193
[26] Lee M, Kim T S and Choi Y S 1997 *J. Non-Cryst. Solids* **211** 143
[27] Kundu D, Honma I, Osawa T and Komiyama H 1994 *J. Am. Ceram. Soc.* **77** 1110
[28] Borrelli N F and Smith D W 1994 *J. Non-Cryst. Solids* **180** 25
[29] Machol J L, Wise F W, Patel R and Tanner D B 1994 *Physica* A **207** 427
[30] Pellegri N, Trbojevich R, De Sanctis O and Kadono K 1997 *J. Sol–Gel Sci. Technol.* **8** 1023